Fluorescence correlation spectroscopy investigation of a GFP mutant-enhanced cyan fluorescent protein and its tubulin fusion in living cells with two-photon excitation

Zifu Wang
Beckman Laser Institute
University of California at Irvine
Irvine, California 92612

Jagesh V. Shah
Ludwig Institute for Cancer Research
University of California at San Diego
La Jolla, California 92093

Zhongping Chen
Chung-Ho Sun
Beckman Laser Institute
University of California at Irvine
Irvine, California 92612

Michael W. Berns
University of California at Irvine
Beckman Laser Institute and
   Department of Biomedical Engineering
Irvine, California 92612
   and
University of California at San Diego
Department of Bioengineering
La Jolla, California 92093

Abstract. This study investigates the feasibility of using the enhanced cyan mutant of green fluorescent protein (ECFP) as a probe for two-photon fluorescence correlation spectroscopy (FCS). Molecular dynamics and other properties of ECFP and an ECFP-tubulin fusion protein were investigated in living *Potorous tridactylis* (PTK2) cells. ECFP has high molecular brightness in the nucleus ($\eta = 3.3$ kcpsm) and in the cytoplasm (3.2 kcpsm) under our experimental conditions. The diffusion constants of ECFP were determined to be 20 ± 7 $\mu m^2/s$ in the nucleus and 21 ± 8 $\mu m^2/s$ in the cytoplasm. ECFP has stable molecular characteristics with negligible photobleaching and photodynamic effects in our measurements. At the highest concentration of monomer ECFP (425 nM) the amount of dimer ECFP was estimated to be negligible ($\sim$1.8 nM), consistent with our data analysis using a single species model. ECFP-tubulin has a diffusion constant of 6 $\mu m^2/s$ in the living cells. In addition, we demonstrate that analysis of the molecular brightness can provide a new avenue for studying the polymerization state of tubulin. We suggest that the tubulin in the vicinity of the nucleus exists primarily as a heterodimer subunit while those in the area away from the nucleus ($d > 5$ μm) are mostly oligomers. We conclude that ECFP is a useful genetic fluorescent probe for FCS studies of various cellular processes when in fusion to other biomolecules of interest. © *2004 Society of Photo-Optical Instrumentation Engineers.*
[DOI: 10.1117/1.1646416]

Keywords: fluorescence correlation spectroscopy; cyan fluorescent protein; intracellular diffusion; tubulin; microtubule; polymerization state.

Paper 03066 received May 19, 2003; revised manuscript received Jul. 30, 2003; accepted for publication Aug. 1, 2003.

1 Introduction

Fluorescence correlation spectroscopy (FCS) is a powerful tool for studying the dynamic properties of diffusion and chemical reaction rates.[1–3] Subsequent integration of confocal and two-photon techniques significantly increased the signal-to-noise ratio of FCS and reduced the measured volume element to less than one femtoliter.[4–7] These developments in FCS technology have opened the possibility to observe the dynamics and concentrations of macromolecules directly in living cells.[8–16]

The availability of green fluorescent protein (GFP) and its various mutants has greatly expanded the possibilities of studying cellular processes *in vivo*.[17] There has been a growing interest in the expression of GFP and GFP-tagged proteins as unique fluorophores to monitor a wide range of intracellular processes, including gene expression,[18] microtubule formation,[19] the assembly of functional ion channels,[20] and the localization and dynamics of specific proteins.[21] To date,

FCS studies of GFP and its fusion proteins have been reported under *in vitro* and intracellular *in vivo* conditions.[10,12,13,15,16,22–25] In most of these studies, one class of GFP mutants [i.e., enhanced green fluorescent protein (EGFP)] was mainly chosen for FCS studies of its molecular dynamics as well as other photophysical properties. Few FCS studies have been reported on other classes of mutants of GFP. The photophysics and photochemistry of other GFP mutants might be surprisingly different and complex as indicated by a study of yellow fluorescent protein (YFP) mutants.[24] To expand the availability of intracellular fluorophores, especially those with genetic tags, it is important to study and characterize the dynamics, thermodynamics, and photophysics of other GFP mutants in the context of FCS measurements.[26] In the present study we characterize the molecular dynamics, molecular brightness, and other molecular properties of one of the GFP mutants, enhanced cyan fluorescent protein (ECFP), specifically in the context of the intracellular environments. The fluorescence (or concentration) fluctuations of a molecular system are the key observable in

Address all correspondence to Dr. Zifu Wang. Current address: Developmental Biology Center, University of California, Irvine, CA 92697, Tel: 949-824-7859; Fax: 949-824-8413; E-mail: zifu@uci.edu

FCS rather than the total amount of measured fluorescence. It has been shown that the crucial parameter for the control of systematic noise is the number of photons per sampling period that can be collected per single observed molecule η (molecular brightness, cpsm) which depends directly on instrumental configuration (i.e., excitation intensity, optics configuration, detector efficiency, etc.) as well as the intrinsic emission properties of the fluorescent molecule.[27] In cellular applications of FCS, the excitation powers have to be kept low enough not to endanger the cell or interfere with its functions and to prevent the dyes from photobleaching. Therefore, it is crucial that the ECFP molecule has high molecular brightness to facilitate intracellular FCS studies. It is also of interest to know if ECFP is sensitive to photobleaching even at low laser power (<2 mW) for live cell measurements because it usually requires data collection of minutes per correlation curve in two-photon FCS measurements.

In the present study, the diffusional mobility, molecular brightness and other molecular properties of ECFP were investigated in cells of the rat kangaroo [*Potorous tridactylis*, (PTK2)] using FCS with two-photon excitation. These cells characteristically remain flat through all phases of the cell cycle, thus affording a clear visualization of the chromosomes, nucleoli, and nuclear envelope.[28,29] We measured the diffusion constants of free ECFP molecules in the nucleus and the cytoplasmic domains as well as its molecular brightness. Our results demonstrate that ECFP is a photochemically and photophysically stable fluorophore with a high molecular brightness. At the highest cellular concentration of ECFP molecules, the amount of ECFP dimer is estimated to be extremely low and its effects on FCS measurements were negligible.

To further test the capability of ECFP as a fluorophore for broad biological applications studied by FCS with two-photon excitation, we have investigated the diffusional mobility of ECFP-tubulin fusion protein at various locations in the cytoplasm of PTK2 cells. Tubulin is the protein component of microtubules and composed of a heterodimer of two closely related proteins called α and β tubulin. This heterodimer is considered the basic subunit to form microtubule. Generally, microtubules exist as single filaments within a cell which radiate from the centrosome close to the nucleus outward throughout the cell. Many microtubule functions are based on tubulin's ability to polymerize and depolymerize readily. Extensive studies on the microtubule dynamics have been conducted under both *in vitro* and *in vivo* conditions, in particular, the mechanism of dynamic instability of single microtubules.[30–32] However, significant questions still remain with respect to our understanding of microtubule dynamic instability.[32] In the present study, we measured the diffusional mobility of the ECFP tubulin fusion in live cells because this dynamic property provides unique information for the studies on microtubule dynamics. In addition, we demonstrate that analysis of the molecular brightness based on the FCS data can provide a new avenue for studying the polymerization state of the tubulin.

We conclude that the ECFP protein molecule in conjunction with FCS can serve as a useful probe for studying various intracellular processes and intracellular environmental properties.

2 Materials and Methods

2.1 Expression and Purification of Recombinant ECFP Protein

The ECFP gene from the ECFP–N1 plasmid (Clontech, CA) was cut out and ligated into the pET30b bacterial expression vector (Stratagene) that has an N-terminal six Histidine tag. E. coli bacteria of strain BL21(DE3) were transformed with the ECFP expression vector, grown to an optical density of 0.6 and then induced with 1 mM IPTG for 18 h at 37°. ECFP protein was purified by lysing bacteria in buffer A (0.1 M Hepes pH 7.7) with 1% Triton X-100 and protease inhibitors. The lysate was then subjected to sonication and insoluble material removed by centrifugation. The soluble portion of the lysate was incubated with Ni–NTA–agarose resin to allow binding of the 6-His-ECFP protein. The beads were washed in buffer A with increasing salt concentrations of NaCl and imidazole. Protein was eluted by the addition of buffer A with 150 mM NaCl and 0.5 M imidazole. ECFP protein was dialysed against phosphate buffered saline (10 mM Phosphate buffer pH 7.2, 150 mM NaCl). ECFP protein was stored at −80 C in a solution of 1% bovine serum albumin as a carrier protein.

2.2 Constructs and Cell Lines

Cells and methods of cell culture used in of these studies were from established sublines of the rat kangaroo *Potorous tridactylis*, PTK2.[33] PTK2 cells and derived lines were cultured in MEM-Earle's supplemented with 10% fetal bovine serum, sodium pyruvate and penicillin and streptomycin. Generation of cell lines stably expressing the fluorescent protein ECFP and fusions to human histone 2B and alpha-tubulin were generated by amphotropic retroviral infection.

The cDNA for enhanced cyan fluorescent was excised from the commercially available ECFP–N1 (Clontech, Palo Alto, CA) via an AfeI/MfeI digest. This fragment was ligated into the SnaBI/EcoRI sites of pBABEpuro. The human alpha-tubulin cDNA fused at its N-terminus to the ECFP was excised from a commercially available plasmid (Clontech, Palo Alto, CA) via an AfeI/MfeI digest. This ECFP-tubulin fragment was ligated into the SnaBI/EcoRI sites of pBABEpuro.

The retroviral plasmids containing the fluorescent protein fusions were cotransfected, using the Fugene transfection reagent (Roche Pharmaceuticals, Indianapolis, IN), into 293-GP cells (a human embryonic kidney cell line harboring a portion of the Murine Moloney Leukemia Virus genome) along with a VSV-G pseudotyping plasmid to generate amphotropic virus. Forty-eight hours after transfection, the tissue culture supernatant was collected, filtered, mixed with 8 μg/mL hexadimethrine bromide (Polybrene, Sigma, St. Louis, MO) and 10% of the total filtrate placed onto a subconfluent culture (30%–40%) of PTK2 cells in 35 mm dishes. Forty-eight hours after infection, cells were split and replated in 10 cm dishes and subjected to selection in 2 μg/mL puromycin for 14 days. High expressors (top 10%) were selected by fluorescence-activated cell sorting (FACSVantage, Becton Dickinson, San Jose, CA). Cells were maintained as polyclonal lines exhibiting various levels of fluorescent protein expression.
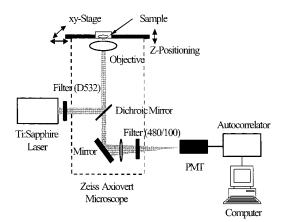
Fig. 1 Experimental setup for two-photon FCS measurements.

2.3 Instrumentation and Measurements

Live cell images were taken on a Nikon Eclipse 300 inverted microscope (Nikon, Melville, NY) using a $60\times$ high numerical aperture (NA 1.4) Plan Apochromat objective. Cells were kept at $35\,°C$ by a stage heater that accommodated glass-bottom 35 mm dishes (Warner Instruments Inc., Hamden, CT). Images were collected by a Photometrics COOLSNAP HQ camera (Roper Scientific, Tuscon, AZ) (gain $=2,10$ MHz) and captured to a computer through the use of the Metamorph software system (Universal Imaging Corp., Downingtown, PA).

FCS with two-photon excitation was performed on a modified Zeiss Axiovert inverted microscope using one of the camera ports for FCS detection (Fig. 1). The collimated beam of a mode-locked tunable Coherent (Palo Alto, CA) Mira 900 titanium–sapphire laser with 76 MHz, 120 fs pulse width was coupled through a Zeiss $63\times$ Plan Apochromat oil immersion objective $(NA=1.4)$. The objective back aperture was slightly overfilled, creating a diffraction-limited focal spot. An excitation wavelength of 800 nm was used for all measurements. The fluorescence from ECFP has an emission peak at 477 nm and was collected with a backscattering geometry and passed through a blue interference filter (HQ480/100M, Chroma Tech., Brattleboro, VT). Photon counts were detected with a GaAsP photomultiplier tube detector (H7421-40, Hamamatsu, Japan). The detector signal was correlated online by a Flex5000/FAST correlator (correlator.com).

PTK2 cells were seeded into 35 mm coverslip-bottom microwells (MatTek Corp., Ashwell, MA) in Phenol Red-free culture medium. The cells were allowed to adhere overnight at $37\,°C$ in a 7.5% CO_2 incubator. From FCS measurements, we determined the concentration of ECFP molecules varying from 66 to 425 nM due to the variation of the expression levels. The laser intensity at the sample was 1.80 mW so as to avoid bleaching the dye and photodamaging the cells. Autocorrelation curves measured from cells were averages of three successive measurements, each 60 s long.

2.4 Data Analysis

Any dynamic process that affects the emission of fluorescent molecules in a solution causes fluctuations in the fluorescence signal $F(t)$ that can be characterized by a normalized autocorrelation function[3]

$$G(\tau)=1+\langle \delta F(t)\delta F(t+\tau)\rangle/\langle F(t)\rangle^2. \qquad (1)$$

In the case of a prolate ellipsoidal Gaussian observation volume in the absence of chemical kinetics, the autocorrelation function has the following analytical form for a single diffusion species
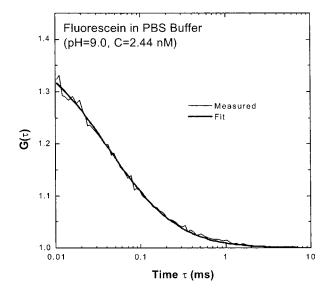
$$G_D(\tau)=1+1/[N(1+\tau/\tau_D)(1+\tau/\omega^2\tau_D)^{0.5}]=1+G_N(\tau), \qquad (2)$$

where τ_D is the characteristic diffusion time during which a molecule resides in the excitation volume with an axial (z_0) to lateral (r_0) dimension ratio ω ($=z_0/r_0$), and $\tau_D=r_0^2/8D$ is defined as the average lateral diffusion time under two-photon excitation for a molecule with diffusion coefficient D through the excitation volume. In the limit $\tau\rightarrow 0$, the mean number of fluorescent molecules N, at concentration C, can be calculated from the normalized initial correlation amplitude, $G_N(\tau\rightarrow 0)$ $=1/N=1/CV$, in a defined excitation volume V.

It has been pointed out by previous investigators applying two-photon FCS that the Gaussian evaluation may not simultaneously reveal consistent absolute values for the independent experimental parameters.[7,10] As a result, a parameter of γ, the inherent volume contrast, is introduced into the calculation of effective focal volume V which in turn modifies the relation between $G_N(0)$ and the average number of molecules in the V as $N==\gamma/G_N(0)$, with γ equal to 0.075 99 for the Gaussian–Lorentzian point spread function (PSF) and 0.3535 for the three-dimensional Gaussian PSF.[34] Thus, the number of photons per molecule per second η (i.e., molecular brightness) can be calculated from the average detected fluorescence intensity with the average number of molecules in the excitation volume. The determination of η is important because it yields absolute values of the detected fluorescence per molecule that are not affected by the local changes in the fluorophore concentration as well as providing a criterion for signal quality. The value of η depends directly on instrumental configuration (i.e., excitation intensity, optics configuration, detector efficiency, etc.) as well as the intrinsic emission properties of the fluorescent molecules. FCS measurements are also susceptible to the background fluorescence (e.g., impure solvent, cellular autofluorescence) and the statistical limitations of intrinsic photon shot noise from the detector. The systematic errors due to the detector after-pulsing usually affect mainly the signal-to-noise at short correlation times ($\leqslant 2$–3 μs), where data quality is critical for resolving fast kinetics but does not affect the analysis of slow dynamics such as diffusion. A constant background signal does not correlate; rather, it affects the correlation function amplitude so that the concentration is overestimated. In the presence of such background, the measured correlation function amplitude must be scaled by $\langle F(t)\rangle^2/[\langle F(t)\rangle-\langle F_{BG}\rangle]^2$, where $\langle F_{BG}\rangle$ is the time-averaged background signal.[27]

2.5 Calibration of the Two-Photon FCS System

To calibrate the system, fluorescence correlation measurements were performed on fluorescein dye molecules in polybutene sulfone (PBS) solution with pH$=9.0$ (Fig. 2) at a concentration of 2.44 nM. Fluorescein is a pH-sensitive dye, and its spectroscopic properties vary drastically from pH 7.5 to 2.
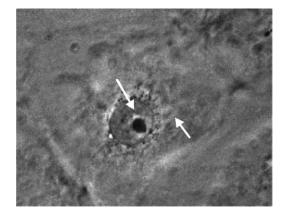
Fig. 2 Autocorrelation curve $G(\tau)$ of fluorescein dyes in PBS solution at concentration of 2.4 nM used for the calibration of our FCS system.

At $pH > 7.5$, fluorescein has a constant quantum yield. The diffusion coefficient of fluorescein is known to be 300 $\mu m^2/s$.[35] We used both the prolate ellipsoidal Gaussian model described by Eq. (2) and a Gaussian–Lorentzian model with LFD Globals Unlimited software (Champaign, IL) to fit our experimental autocorrelation curve.[7] Both models gave a value of 0.30 μm for the lateral dimension r_0 of the excitation volume. The excitation volume can be recovered based on the known parameters of concentration (2.44 nM) and the number of the molecules N in the volume. With the γ of 0.075 59 and $G_N(0) = 0.40$, the average number N of fluorescein molecules in the volume is 0.19, thus we obtained an excitation volume of 0.129 femtoliter.

3   Results

3.1   Intracellular FCS Measurements of Free ECFP

PTK2 cells characteristically remain flat throughout all phases of their cell cycle. Figure 3 shows a cell in interphase that

Fig. 3 A PTK2 cell in interphase with a clear visualization of the nucleoli and nuclear envelope. Arrows indicate the locations where the two-photon FCS measurements were performed inside the nucleus and the cytoplasm, respectively.
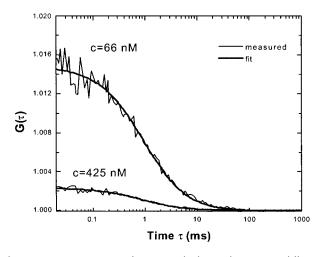
Table 1 FCS analysis of ECFP *in vivo* and *in vitro*.

ECFP	Nucleus (20 cells)	Cytoplasm (10 cells)	Solution (4 positions)
$\langle D \rangle$ ($\mu m^2/s$)	20 ± 7	21 ± 8	82 ± 2
$\langle \eta \rangle$ (cpsm)	3400 ± 100	3200 ± 200	3300 ± 100

offers a clear visualization of the nucleoli and nuclear envelope. Autofluorescence contributions may arise from mobile native fluorophores. It is known that NADH and flavoproteins, mostly localized in the cellular mitochondria, are two main sources of autofluorescence. Because NADH and flavoproteins have typically low fluorescence quantum yields and are easily photobleached, their signal will not correlate during its diffusion through the excitation volume. In this case, the presence of autofluorescence may affect the amplitude of the correlation curve but not its decay parameters,[10] and can be corrected for as a constant background.[36] In the present study, nontransfected cells were measured as a control to account for the cellular autofluorescence background. The intrinsic autofluorescence intensity inside the cells is usually stable as a function of time. The average intensity of the autofluorescence from the measurements on ten cells was 2500 cps and there were no clear correlation curves obtained from these control measurements, indicating that the molecular brightness of the native mobile molecules are low.

During the experiments the sample stage of the microscope was translated to different positions for intracellular measurements. ECFP cells were measured at several randomly selected locations within the nucleus and the cytoplasm in each individual cell. Cells with fluorescence intensity above 10 000 cps were selected for the experiments. In fact, most of the ECFP expressing cells presented fluorescence intensity $\sim 25\,000$ cps which made the background counts a fairly small fraction of the total intensity. In the experiments, the microscope objective was carefully adjusted in the z direction with a resolution of 1 μm to ensure that the focal volume of the laser beam was within the body of the cells in order to prevent the measurements of anomalous subdiffusion of proteins restricted to cell membranes.[10,11] It has been demonstrated that in the absence of photobleaching, the apparent diffusion rate is independent of the illumination intensity.[36–38] To evaluate the effect of photobleaching of ECFP to our recovered diffusion constants, we conducted several FCS measurements in solution with a laser power varying from 1.5 to 5 mW and obtained virtually identical autocorrelation curves. FCS measurements were then performed within a small volume inside the nucleus and the cytoplasm of a cell with a laser power varying from 1.5 to 2.4 mW. Again we obtained identical autocorrelation curves in each domain. This indicates that there is no detectable photobleaching of ECFP within the range of incident laser intensity in our experiments.

Table 1 summarizes the average dynamic and photophysical properties of ECFP recovered from the FCS measurements under both *in vitro* and *in vivo* conditions. The average diffusion constant of ECFP molecules in the nucleus was determined to be 20 ± 7 (std. error) $\mu m^2/s$. Although comparable studies of ECFP in PBS buffer ($D = 82$ $\mu m^2/s$) have shown

Fig. 4 FCS measurements of ECFP inside the nucleus at two different concentrations (66 and 425 nM). Note the difference in the amplitude of the autocorrelation curves at $\tau=0$ $[G(0)]$ due to the difference in concentrations.

Fig. 5 A fluorescence image of a living PTK2 cell shows the intracellular distribution of microtubules with ECFP tagged tubulin. The bright centrosome region is clearly seen in this picture which is within the distance $\sim$5 μm from the nucleus. Scale bar=20 μm.
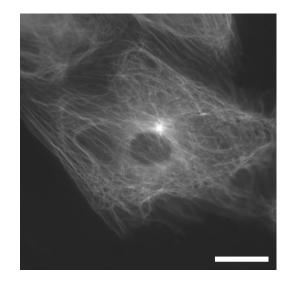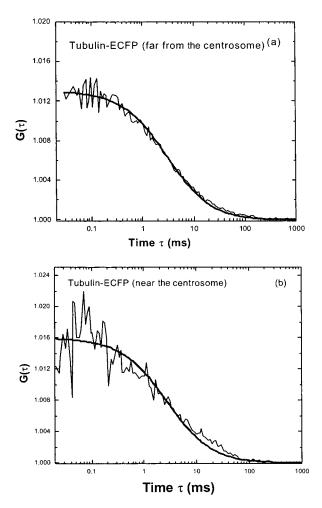
significant differences with ECFP diffusion in the nucleus, diffusion of ECFP in the nucleus can be described by assuming a single diffusing species.[10,16] For comparison, measurements in the cytoplasm were also conducted on ten cells. The recovered average diffusion constant of ECFP is 21 ± 8 (std. error) μm^2/s (Table 1). The average diffusion constant is similar in the nucleus and the cytoplasm. This result was similar to that reported on EGFP previously.[16,39] The concentration of ECFP in the cells varied from 66 to 425 nM (Fig. 4).

To recover the molecular brightness of ECFP in cells, we scaled the measured correlation function amplitude by a factor of $\langle F(t) \rangle^2 / [\langle F(t) \rangle - \langle F_{BG} \rangle]^2$, where the $\langle F_{BG} \rangle$ was equal to 2500 cps. The obtained molecular brightness η of ECFP in the nucleus was 3400 ± 100 cpsm and 3200 ± 200 cpsm in the cytoplasm, very close to the results from FCS measurements of ECFP in solution (3300 ± 100 cpsm). This also indicates that, after the autofluorescence was corrected for as a constant background, the contributions of the mobile native fluorophores from the cells to the measured autocorrelation curves are negligible because these native fluorophores typically have low fluorescence quantum yields, which is consistent with the previous observation.[36]

Because the value of the η reflects the detection efficiency of a FCS system, it would be interesting to compare our results with published data. For this purpose, we conducted an *in vitro* FCS measurement of EGFP in buffer solution with two-photon excitation at 850 nm because the η value of EGFP has been determined in previous studies.[10,16] The η value of EGFP determined with our FCS system is 1500 ± 200 cpsm which is very close to that determined in a previous study of EGFP.[16] This indicates that our FCS system has a high detection efficiency similar to that of the system used in the previous study.

3.2 Intracellular Investigation of ECFP Tubulin Fusion

The distribution of microtubules in the ECFP tubulin cells was observed with a conventional epifluorescence microscope (Fig. 5). We observed that the centrosome, or the microtubule

organizing center, was located near the nucleus within a distance of about 5 μm. To evaluate the effects of the compact centrosome structures with respect to tubulin, we conducted FCS measurements at several randomly selected locations in the vicinity of the nucleus ($d<5 \mu$m) and obtained dramatically different results (Fig. 6). At certain locations there were simply no clear autocorrelation curves despite the strong fluorescence signal, indicating that it was the place where most of the tubulin molecules were insoluble and integrated into the microtubule-based structures. At other locations away from the centrosome, the quality of the measured autocorrelation function curves varied as shown in Fig. 6 with distance from the centrosome. The autocorrelation curves with good quality could be fit using a single species model.

Table 2 summarizes the average diffusion constants of tubulin. Due to the variation in the quality of the FCS measurements in the vicinity of the nucleus, we chose the measurements with clear autocorrelation curves for determining the diffusion constant. The average diffusion constant of tubulin in the vicinity of the nucleus was determined to be $6.2 \pm 1.5 \mu$m^2/s. FCS measurements were also conducted in the area away from the nucleus ($d>5 \mu$m) where there is a lower density of microtubule scaffolding. The diffusion constant was determined to be $6.0 \pm 1.5 \mu$m^2/s.

We also calculated the molecular brightness of tubulin at various locations (Table 2). We obtained a value of 3400 ± 500 cpsm in the vicinity of the nucleus ($d<5 \mu$m). Away from the nucleus we obtained larger brightness values. From the measurements in ten cells on the randomly selected locations within the area between 5 and 20 μm from the nucleus, the average value of the brightness is about twice that in the vicinity of the nucleus (6400 ± 300 cpsm). The measurements at the locations greater than 20 μm from the nucleus were not chosen for the calculation of the molecular brightness because the thickness of the cells became thinner than the axial dimension of the excitation volume of the laser beam, which may

Fig. 6 Two FCS measurements conducted in the vicinity of the nucleus in a living PTK2 cell expressing ECFP-tubulin. (a) Far from the centrosome. (b) Near the centrosome. The quality of the autocorrelation curves changes with its distance from the centrosome region.

produce errors in estimating the number of the fluorophores in the volume.

Tubulin protein is expected to be almost exclusively in the cytoplasm. However, our FCS measurements conducted inside the nucleus indicate that a considerable amount of tubulin resides inside the nucleus (Fig. 7). The average concentration of the protein in the nucleus is about 50 nM. This was comparable to the concentration in the cytoplasm away from the nucleus. The average diffusion constant is 5.7 ± 0.7 $\mu m^2/s$ recovered from our measurements on ten cells.

Table 2 FCS analysis of ECFP fusion tubulin molecule in the cytoplasm of PTK2.

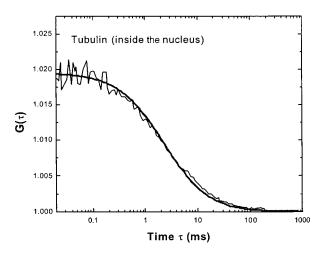| Tubulin-ECFP	Near the nucleus (10 cells) ($d < 5$ μm)	Far from the nucleus (10 cells) (5 μm $< d < 20$ μm)
$\langle D \rangle$ ($\mu m^2/s$)	6.2 ± 1.5	6.0 ± 1.5
$\langle \eta \rangle$ (cpsm)	3400 ± 500	6400 ± 300

Fig. 7 A FCS measurement obtained inside the nucleus of a living PTK2 cell expressing ECFP-tubulin.

4 Discussion

In this study FCS measurements with two-photon excitation were performed to investigate the intracellular molecular dynamics, molecular brightness as well as other photophysical properties of ECFP. We also investigated the diffusional mobility and the molecular brightness of an ECFP tubulin fusion protein in living cells.

4.1 ECFP Does Not Exhibit Proton-Driven Flickering

Optical excitation-driven intramolecular dynamics of some GFP mutants (e.g., EGFP, S65T, and YFP) have been studied, where submillisecond flicker was observed due to proton displacement between the protonated (dark) and unprotonated (bright) states of the chromophore through the hydroxyl groups which provide H^+ binding sites.[22,24] To the best of our knowledge, such phenomena have not been reported for ECFP, presumably because of the difference in the structure of its chromophore, where substitution of Trp for Tyr66 produces a new chromophore with an indole instead of a phenol or phenolate existing in the mutants investigated previously.[17,40] The indole does not possess a protonatable hydroxyl group. A previous measurement on a mutant Y66W of CFP has demonstrated that a chromophore with an indole structure did not present fluorescence "flickering" dynamics.[22] In our measurements, we did not observe changes in the shape of autocorrelation curves of the ECFP molecules both in buffer solution and in living cells at various laser intensities (1.5–5.0 mW) and acquisition times under our experimental conditions. We conclude that ECFP molecules are photochemically stable under the experimental conditions and our measured FCS results reflect the fluctuation of fluorescence signals due to the mobile movements of ECFP molecules.

4.2 Effects of Dimerization of ECFP

It has been pointed out that the crystal structures of GFP as well as GFP mutants in solution at high concentration have the tendency to form twofold symmetric dimers.[41,42] This dimerization of the protein has been a concern in other studies where it is crucial to ensure the monomer status of GFP

molecules.[43] In the present study, the concentration of ECFP is up to 425 nM in the cells. Even though at such high concentration the measured autocorrelation curves can still be fit with a single species model, the effects of dimerization of the protein on our measurements need to be addressed.

The dissociation constants (K_D) of both GFP and YFP have been determined to be approximately 100 μM indicating that the proteins have a very weak chemical affinity.[43,44] Because ECFP and these two proteins have a very similar molecular structure, we expect that they have very similar chemical properties in terms of the chemical affinity and we expect the dissociation constant of ECFP to be around 100 μM.[45] At the highest concentration of ECFP in the present study (425 nM) (Fig. 4), the concentration of the dimer is estimated to be 1.8 nM leading to a ratio of 236:1 between the monomer and the dimer. This indicates that with an average of 33 monomer molecules in our excitation volume there is only 0.14 dimer molecules of ECFP at the same time, therefore, the contribution of the dimer molecules of ECFP to our measurements is negligible. Furthermore, if all ECFP is in single molecular form, the fluorescence intensities should be proportional to the corresponding concentrations. We chose two measurements of ECFP with concentrations of 66 and 425 nM as shown in Fig. 4. The ratio between the two concentrations is 6.4. The corresponding background adjusted signal intensities are 114 900 and 17 920 cps and the ratio between the intensities is also 6.4, indicating that the ECFP molecules are essentially a single form of the monomer. Therefore, we are able to rule out the possibility of the dimer contribution to the measurements. Our results indicate that the ECFP molecule is remarkably inert and our FCS measurements reflect the free diffusion of the monomer ECFP molecules in the intracellular environment, which is consistent with previous *in vivo* observations on EGFP molecules.[10,16,39]

4.3 *In vivo Molecular Brightness and Dynamics of ECFP*

The molecular brightness recovered from the measurements of ECFP in cells is very similar to that from in vitro solutions (Table 1). This is consistent with our understanding of the structure of ECFP where the chromophore is protected from the influences of the external environment. Under our experimental conditions, ECFP molecule exhibits high molecular brightness ($>$3000 cpsm) that greatly facilitates the FCS measurements with two-photon excitation.

Diffusion constants of ECFP molecules were measured in the intracellular environment and compared to those measured in solutions (Table 1). The mobility of the molecules was slowed about by a factor of 4 in cells. Because the ECFP molecule is chemically stable, molecular crowding and collisional interactions with other cellular components are likely responsible for the slowed diffusion in cells. We note the slight difference in diffusion rates of ECFP relative to that of EGFP as observed in previous observations.[10,16] This may be due to different intracellular environments in different cell lines. The similar diffusion constants of ECFP in the nucleus and the cytoplasm indicate that the intracellular environment is homogeneous in terms of the diffusion of small molecules like ECFP, although the actual architectures of the nucleus and the cytoplasm are different.

4.4 *Intracellular Molecular Dynamics of Tubulin Molecule*

One of the important factors affecting microtubule dynamics is how easily a microtubule fiber can capture a tubulin subunit from the free tubulin pool during the process of polymerization, which is closely related to the translational mobility of those free tubulin in the cytoplasmic area.[46] Knowledge of the diffusion of tubulin *in vivo* will provide unique and important information to enhance our understanding of microtubule dynamics. To further test the capability of ECFP as a fluorophore for broad biological applications studied by two-photon FCS, we measured the diffusion constant of ECFP tubulin at various locations in living PTK2 cells (Table 2). Our results are identical to the results from a previous in vivo study (diffusion constant 6 μm^2/s) of tubulin in the cytoplasm of eggs and embryos of the sea urchin using fluorescence recovery after photobleaching (FRAP) technique, where fluorescein-labeled tubulin was injected into the eggs and embryos.[47] The *in vitro* diffusion constant of tubulin in buffer solution is about 43 μm^2/s,[48] suggesting that the cytoplasmic viscosity of PTK2 cells sensed by tubulin is about seven times the viscosity of the buffer solution.

The variation in the FCS measurements performed in the vicinity of the nucleus reveals the local effects of the microtubule cytoskeleton on the diffusional mobility of tubulin. At the centrosome, most of the tubulin is polymerized so there are few free tubulin molecules, which results in no correlation curves for the FCS measurements. Away from the centrosome, the density of the microtubule fibers decreases and FCS measurements can be performed on the free tubulin pool, where FCS data with good quality can be obtained [Fig. 6(a)].

The observation of free tubulin inside the nucleus is interesting. The concentration of free tubulin in the nucleus is comparable to that at locations distant from the nucleus ($d > 5 \mu$m). The diffusion constant is basically the same as in the cytoplasm. It is not known how this tubulin enters the nucleus and what its nuclear functions may be.

4.5 *Oligomerization State of Tubulin Molecule*

Knowledge of the oligomerization state of tubulin is crucial for understanding the mechanism of the dynamic instability because it provides information on the basic molecular building blocks of microtubules. Previous reports suggest that tubulin exists primarily as dimers and small oligomers based on the analysis of measured diffusion constants of tubulin in squid giant axons or eggs and embryos of the sea urchins.[47–49] However, because the diffusion constant varies with the cube root of the molecular weight to a first approximation,[47] it is difficult to resolve the oligomerization state of the small oligomers based on the measured diffusion constant.

In the present study, each α-tubulin is genetically tagged with an ECFP molecule so each tubulin heterodimer, the basic subunit for microtubules, carries one ECFP. The molecular brightness of free ECFP has been recovered both *in vitro* and *in vivo* and was discussed in the previous sections. We believe that the analysis of the molecular brightness can provide a more accurate picture of the oligomerization state of tubulin. The molecular brightness of ECFP tagged tubulin in the area near the nucleus is 3400$\pm$500 cpsm that is very close to the brightness of a single free ECFP. Considering the special po-

sition of the chromophore in the center of the β-barrel structure of ECFP, the environmental effects on the optical properties of the chromophore should be weak. In this context, we suggest that the tubulin near the nucleus exists primarily in the form of a heterodimer, the basic subunit. On the other hand, the brightness of the tubulin in the area away from the nucleus is about twice that near the nucleus (6400 ± 300 cpsm), indicating that most of the tubulin in this area is in the form of small oligomers with two subunits. We note that the immobile tubulin-ECFP could also influence the FCS determination of the molecular brightness of ECFP in living cells in addition to the influence of the autofluorescence background. To account for these background effects, recently developed photon counting histogram[50,51] and fluorescence intensity distribution analysis[52,53] will be used in the future studies to further resolve the oligomerization state of tubulin.

In summary, this study clearly demonstrates that two-photon FCS can be used to measure ECFP and its fusion molecules in living cells. Under our experimental conditions, ECFP presents stable photochemical characteristics so that photobleaching and photodynamic effects in FCS measurements are negligible. We demonstrate that ECFP has a high molecular brightness and its intracellular mobility is similar to other GFP mutants mainly due to the overall similar structures that determine their photophysics and molecular dynamics. Our calculations indicate that the amount of the ECFP dimer is extremely low even at the highest concentration of the protein in this study, therefore, the effects of dimerization on our measurements are negligible. Our *in vivo* FCS studies of the molecular dynamics of the ECFP tubulin fusion present an identical diffusion constant to a previous result obtained with the FRAP technique.[47] In addition, we demonstrate that analysis of the molecular brightness based on the FCS can provide a new avenue for studying the oligomerization state of tubulin, which is vital to understanding the mechanism of dynamic instability of microtubules *in vivo*. We conclude that ECFP is a very useful fluorescent probe for FCS studies of various cellular processes when fused to other biomolecules of interest.

Acknowledgments

References

1. D. Magde, E. Elson, and W. W. Webb, "Thermodynamic fluctuations in a reacting system-measurements by fluorescence correlation spectroscopy," *Phys. Rev. Lett.* **29**, 705–708 (1972).
2. D. Magde, E. L. Elson, and W. W. Webb, "Fluorescence correlation spectroscopy. II. An experimental realization," *Biopolymers* **13**, 29–61 (1974).
3. E. L. Elson and D. Magde, "Fluorescence correlation spectroscopy I. Conceptual basis and theory," *Biopolymers* **13**, 1–27 (1974).
4. R. Rigler, U. Mets, J. Widengren, and P. Kask, "Fluorescence correlation spectroscopy with high count rate and low background: analysis of translational diffusion," *Eur. Biophys. J.* **22**, 169–175 (1993).
5. D. E. Koppel, F. Morgan, A. E. Cowan, and J. H. Carson, "Scanning concentration correlation spectroscopy using the confocal laser microscope," *Biophys. J.* **66**, 502–507 (1994).
6. H. Qian and E. L. Elson, "Analysis of confocal laser-microscope optics for 3-D fluorescence correlation spectroscopy," *Appl. Opt.* **30**, 1185–1195 (1991).
7. K. M. Berland, P. T. C. So, and E. Gratton, "Two-photon fluorescence correlation spectroscopy: method and application to the intracellular environment," *Biophys. J.* **68**, 694–701 (1995).
8. R. Brock, M. A. Hink, and T. M. Jovin, "Fluorescence correlation microscopy of cells in the presence of autofluorescence," *Biophys. J.* **75**, 2547–2557 (1998).
9. J. C. Politz, E. S. Browne, D. E. Wolf, and T. Pederson, "Intranuclear diffusion and hybridization state of oligonucleotides measured by fluorescence correlation spectroscopy," *Proc. Natl. Acad. Sci. U.S.A.* **95**, 6043–6048 (1998).
10. P. Schwille, U. Haupts, S. Maiti, and W. W. Webb, "Molecular dynamics in living cells observed by fluorescence correlation spectroscopy with one- and two-photon excitation," *Biophys. J.* **77**, 2251–2265 (1999).
11. P. Schwille, J. Korlach, and W. W. Webb, "Fluorescence correlation spectroscopy with single-molecule sensitivity on cell and model membranes," *Cytometry* **36**, 176–182 (1999).
12. R. Brock, G. Vamosi, G. Vereb, and T. M. Jovin, "Rapid characterization of green fluorescent protein fusion proteins on the molecular and cellular level by fluorescence correlation microscopy," *Proc. Natl. Acad. Sci. U.S.A.* **96**, 10123–10128 (1999).
13. M. Wachsmuth, W. Waldeck, and J. Langowski, "Anomalous diffusion of fluorescent probes inside living cell nuclei investigated by spatially resolved fluorescence correlation spectroscopy," *J. Mol. Biol.* **298**, 677–689 (2000).
14. G. Boonen, A. Pramanik, R. Rigler, and H. Haberlein, "Evidence for specific interactions between kavain and human cortical neurons monitored by fluorescence correlation spectroscopy," *Planta Med.* **66**, 7–10 (2000).
15. R. H. Kohler, P. Schwille, W. W. Webb, and M. R. Hanson, "Active protein transport through plastid tubules: velocity quantified by fluorescence correlation spectroscopy," *J. Cell. Sci.* **113**, 3921–3930 (2000).
16. Y. Chen, J. D. Müller, Q. Ruan, and E. Gratton, "Molecular brightness characterization of EGFP *in vivo* by fluorescence fluctuation spectroscopy," *Biophys. J.* **82**, 133–144 (2002).
17. R. Y. Tsien, "The green fluorescent protein," *Annu. Rev. Biochem.* **67**, 509–544 (1998).
18. Y. Wang, Y. Yu, S. Shabahang, G. Wang, and A. A. Szalay, "Renilla luciferase-Aequorea GFP (Ruc-GFP) fusion protein, a novel dual reporter for real-time imaging of gene expression in cell cultures and in live animals," *Mol. Gen. Genomics.* **268**, 160–168 (2002).
19. J. M. Askham, K. T. Vaughan, H. V. Goodson, and E. E. Morrison, "Evidence that an interaction between EB1 and p150(glued) is required for the formation and maintenance of a radial microtubule array anchored at the centrosome," *Mol. Biol. Cell* **13**, 3627–3645 (2002).
20. I. Szabo, A. Negro, P. M. Downey, M. Zoratti, F. Lo Schiavo, and G. M. Giacometti, "Temperature-dependent functional expression of a plant K(+) channel in mammalian cells," *Biochem. Biophys. Res. Commun.* **274**, 130–135 (2000).
21. B. J. Howell, D. B. Hoffman, G. Fang, A. W. Murray, and E. D. Salmon, "Visualization of Mad2 dynamics at kinetochores, along spindle fibers, and at spindle poles in living cells," *J. Cell Biol.* **150**, 1233–1249 (2000).
22. U. Haupts, S. Maiti, P. Schwille, and W. W. Webb, "Dynamics of fluorescence fluctuations in green fluorescent protein observed by fluorescence correlation spectroscopy," *Proc. Natl. Acad. Sci. U.S.A.* **95**, 13573–13578 (1998).
23. E. Guiot, M. Enescu, B. Arrio, G. Johannin, G. Roger, S. Tosti, F. Tfibel, F. Mérola, A. Brun, P. Georges, and M. P. Fontaine-Aupart, "Molecular dynamics of biological probes by fluorescence correlation microscopy with two-photon excitation," *J. Fluoresc.* **10**, 413–419 (2000).
24. P. Schwille, S. Kummer, Ahmed A. Heikal, W. E. Moerner, and W. W. Webb, "Fluorescence correlation spectroscopy reveals fast optical excitation-driven intramolecular dynamics of yellow fluorescent proteins," *Proc. Natl. Acad. Sci. U.S.A.* **97**, 151–156 (2000).
25. Q. Ruan, Y. Chen, E. Gratton, M. Glaser, and W. W. Mantulin, "Cel-

lular characterization of adenylate kinase and its isoform: two-photon excitation fluorescence imaging and fluorescence correlation spectroscopy," *Biophys. J.* **83**, 3177–3187 (2002).

26. W. W. Webb, "Fluorescence correlation spectroscopy: inception, biophysical experimentations, and prospectus," *Appl. Opt.* **40**, 3969–3983 (2001).

27. D. E. Kopple, "Statistical accuracy in fluorescence correlation spectroscopy," *Phys. Rev. A* **10**, 1938–1945 (1974).

28. M. W. Berns, J. Aist, J. Edwards, K. Strahs, J. Girton, P. McNeill, J. B. Rattner, M. Kitzes, M. Hammer-Wilson, and L. H. Liaw, "Laser microsurgery in cell and developmental biology," *Science* **213**, 505–513 (1981).

29. M. W. Berns, Z. Wang, A. Dunn, V. Wallace, and V. Venugopalan, "Gene inactivation by multiphoton-targeted photochemistry," *Proc. Natl. Acad. Sci. U.S.A.* **97**, 9504–9507 (2000).

30. T. Mitchison and M. Kirschner, "Dynamic instability of microtubule growth," *Nature (London)* **312**, 237–242 (1984).

31. T. Mitchison and M. Kirschner, "Microtubule assembly nucleated by isolated centrosomes," *Nature (London)* **312**, 232–237 (1984).

32. A. Desai and T. J. Mitchison, "Microtubule polymerization dynamics," *Annu. Rev. Cell Dev. Biol.* **13**, 83–117 (1997).

33. P. A. McNeill and M. W. Berns, "Chromosome behavior after laser microirradiation of a single kinetochore in mitotic PtK2 cells," *J. Cell Biol.* **88**, 543–553 (1981).

34. Y. Chen, J. D. Mülle, K. M. Berland, and E. Gratton, "Fluorescence fluctuation spectroscopy," *Methods* **19**, 234–252 (1999).

35. N. L. Thompson, *Topics in Fluorescence Spectroscopy*, J. R. Lakowicz, Ed., Vol. 1, pp. 337–378, Plenum, New York (1991).

36. S. T. Hess, S. Huang, A. A. Heikal, and W. W. Webb, "Biological and chemical applications of fluorescence correlation spectroscopy: a review," *Biochemistry* **41**, 697–705 (2002).

37. J. Widengren and R. Rigler, "Mechanisms of photobleaching investigated by fluorescence correlation spectroscopy," *Bioimaging* **4**, 149–157 (1996).

38. J. Mertz, "Molecular photodynamics involved in multi-photon excitation fluorescence microscopy," *Eur. Phys. J. D* **3**, 53–66 (1998).

39. E. O. Potma, W. P. de Boeij, L. Bosgraaf, J. Roelofs, P. J. M. van Haastert, and D. A. Wiersma, "Reduced protein diffusion rate by cytoskeleton in vegetative and polarized *dictyostelium* cells," *Biophys. J.* **81**, 2010–2019 (2001).

40. R. Heim, D. C. Prasher, and R. Y. Tsien, "Wavelength mutations and posttranslational autoxidation of green fluorescent protein," *Proc. Natl. Acad. Sci. U.S.A.* **91**, 12501–12504 (1994).

41. F. Yang, L. G. Moss, and G. N. Phillips, Jr., "The molecular structure of green fluorescent protein," *Nat. Biotechnol.* **14**, 1246–1251 (1996).

42. K. K. Jensen, L. Martini, and T. W. Schwartz, "Enhanced fluorescence resonance energy transfer between spectral variants of green fluorescent protein through zinc-site engineering," *Biochemistry* **40**, 938–945 (2001).

43. D. A. Zacharias, J. D. Violin, A. C. Newton, and R. Y. Tsien, "Partitioning of lipid-modified monomeric GFPs into membrane microdomains of live cells," *Science* **296**, 913–916 (2002).

44. G. N. Phillips, Jr., "Structure and dynamics of green fluorescent protein," *Curr. Opin. Struct. Biol.* **7**, 821–827 (1997).

45. R. Y. Tsien (personal communication).

46. D. J. Odde, "Estimation of the diffusion-limited rate of microtubule assembly," *Biophys. J.* **73**, 88–96 (1997).

47. E. D. Salmon, W. M. Saxton, R. J. Leslie, M. L. Karow, and J. R. McIntosh, "Diffusion coefficient of fluorescein-labeled tubulin in the cytoplasm of embryonic cells of a sea urchin: video image analysis of fluorescence redistribution after photobleaching," *J. Cell Biol.* **99**, 2157–2164 (1984).

48. J. A. Galbraith, T. S. Reese, M. L. Schlief, and P. E. Gallant, "Slow transport of unpolymerized tubulin and polymerized neurofilament in the squid giant axon," *Proc. Natl. Acad. Sci. U.S.A.* **96**, 11589–11594 (1999).

49. S. Terada, M. Kinjo, and N. Hirokawa, "Oligomeric tubulin in large transporting complex is transported via kinesin in squid giant axons," *Cell* **103**, 141–155 (2000).

50. Y. Chen, J. D. Muller, S. Y. Tetin, J. D. Tyner, and E. Gratton, "Probing ligand protein binding equilibria with fluorescence fluctuation spectroscopy," *Biophys. J.* **79**, 1074–1084 (2000).

51. J. S. Eid, J. D. Muller, and E. Gratton, "Data acquisition card for fluctuation correlation spectroscopy allowing full access to the detected photon sequence," *Rev. Sci. Instrum.* **71**, 361–368 (2000).

52. P. Kask, K. Palo, D. Ullmann, and K. Gall, "Fluorescence-intensity distribution analysis and its application in biomolecular detection technology," *Proc. Natl. Acad. Sci. U.S.A.* **96**, 13756–13761 (1999).

53. P. Kask, K. Palo, N. Fay, L. Brand, U. Mets, D. Ullmann, J. Jungmann, J. Pschorr, and K. Gall, "Two-dimensional fluorescence intensity distribution analysis: theory and applications," *Biophys. J.* **78**, 1703–1713 (2000).